#### On-Chip Si<sub>3</sub>N<sub>4</sub> Spatial Heterodyne Fourier Transform Spectrometer for the Optical Window in Biological Tissue

Kyoung Min Yoo<sup>1</sup>, Ray T. Chen<sup>1,2</sup>

<sup>1</sup>Department of Electrical and Computer Engineering, The University of Texas at Austin, 10100 Burnet Rd. Austin, TX, 78758, USA.

<sup>2</sup>Omega Optics Inc., 8500 Shoal Creek Blvd., Bldg. 4, Suite 200, Austin, TX, 78757, USA.

Author e-mail address: yoo\_eb@utexas.edu, chenrt@austin.utexas.edu

**Abstract:** We designed and demonstrated an on-chip Fourier transform spectrometer on  $Si_3N_4$ -on- $SiO_2$  using an array of Mach-Zehnder interferometers (MZIs) for  $\lambda = 600 \sim 1000$  nm. The retrieval of an input spectrum is demonstrated by the interconnect simulation. © 2021 The Author(s)

Fourier transform spectroscopy (FTS) is a technique that measures the spectrum with the interference of light instead of dispersion, offering the advantages including high optical throughput and multiplex advantage, in turn, larger signal-to-noise ratio compared to grating-based spectrometers [1-3]. Also, a non-invasive in vivo diffuse optical characterization of human tissues using optical spectroscopy to assess mean absorption and reduced scattering spectra in the wavelength range of 600-1200 nm opens a new possibility of monitoring various vital signatures of users [4]. Especially, the blood oxygen levels can be evaluated by monitoring the levels of HbO<sub>2</sub> and Hb, which have absorption peaks at  $\lambda = 905$  nm and  $\lambda = 750$  nm [5]. In this paper, we designed and demonstrated an on-chip FTS consists of an array of MZI with linearly increasing optical path delays, also called a spatial heterodyne FTS (SHFTS) at the human body transparent wavelength region (600-1000 nm). It has been demonstrated that the SHFTS produces a spatial interference pattern at their outputs and the input spectrum can be retrieved using Fourier analysis in the data processing stage, allowing the acquisition of the entire interferogram in a single capture [1-3]. We chose the Si<sub>3</sub>N<sub>4</sub> waveguide with SiO<sub>2</sub> claddings due to the low material absorption losses in the human tissue optical window [6]. The schematic illustrations of the proposed SHFTS structure and Si<sub>3</sub>N<sub>4</sub> strip waveguide are shown in Fig. 1. (a) and (b).

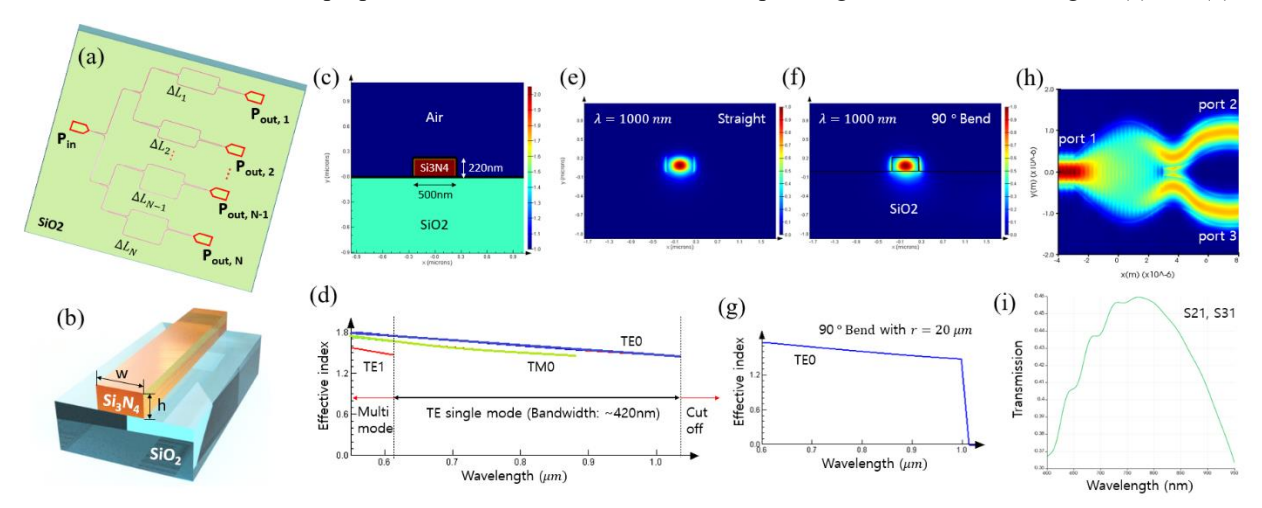


Fig. 1. (a) Schematic structure of the SHFTS consists of MZI array. (b) Schematic of the  $Si_3N_4$  strip waveguide on  $SiO_2$  bottom cladding. (c) Refractive index profile of the designed strip waveguide (w=500nm, h=220nm) and (d) the effective index of guiding modes as a function of wavelength. (e) Cross-section of the fundamental TE mode profile in straight waveguide and (f) in 90° bend. (g) Effective index of fundamental TE mode in 90° bent waveguide with r=20 $\mu$ m. (h) E-field and (i) S-parameters of optimized Y-branch structure using particle-swarm algorithm.

First, broadband single-mode  $Si_3N_4$  waveguide is designed to cover the 600-1000nm wavelength range. The height (h) and width (w) of the  $Si_3N_4$  waveguide are determined by sweeping the refractive index to ensure the single-mode operation using Lumerical Mode simulation. The refractive index profile of optimized strip waveguide with h=220nm and w=500nm and the effective index of guiding modes as a function of wavelength are shown in Fig. 1. (c) and (d), which show that the designed strip waveguide covers the single-mode operation range from 620nm to 1040nm. Also, the low-loss waveguide bend and Y-branch are designed to guide the single TE mode. By sweeping the bending radius from 1  $\mu m$ , we found that the minimum bend radius of 20  $\mu m$  is required to guide the fundamental TE mode up to  $\lambda = 1000 \ nm$ . The fundamental TE mode profiles of the straight waveguide and bent waveguide are shown in

JTu3A.122.pdf CLEO 2021 © OSA 2021

Fig. 1. (e) and (f), which have ~99% overlap mode matching, in turn, the total 90° bend loss was <0.03 dB. The Y-branch is optimized through the built-in particle swarm optimization algorithm in Lumerical Mode and FDTD to achieve the minimum loss across the wavelength range from 600nm to 1000 nm. The top-view electrical field and S-parameters of each port of the designed Y-branch are shown in Fig. 1. (h) and (i), which indicate that the total Y-branch losses at the wavelengths of 800 nm and 900 nm are ~0.4 dB and ~0.9 dB, respectively.

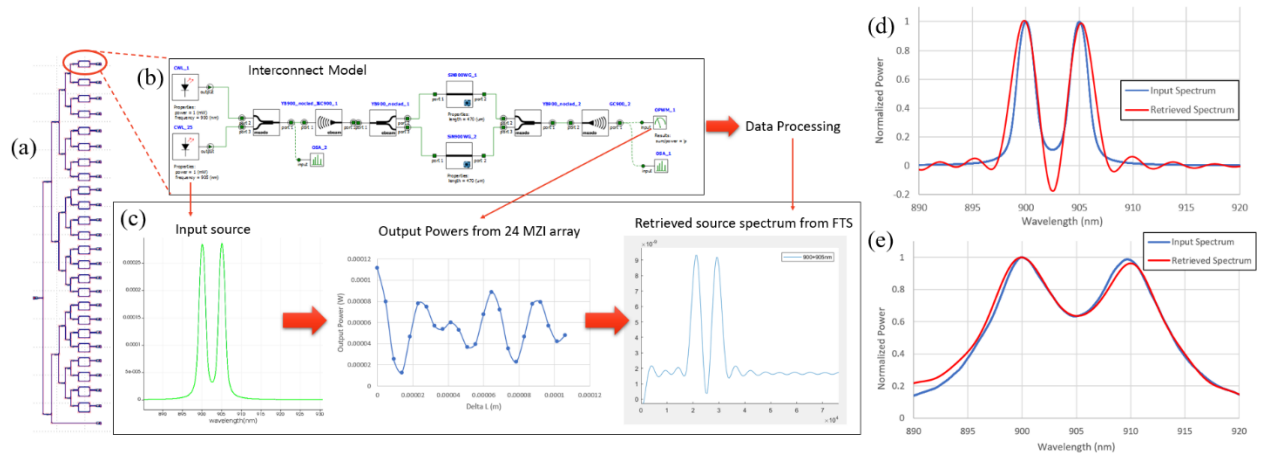


Fig. 2. (a) SHFTS design floor plan. (b) Compact Interconnect model for each MZI. (c) Overall FTS operation procedure. Input and retrieved spectrum from FTS with various input sources: (d) Peaks are separated by 5 nm ( $\lambda$ =900 nm and 905 nm). (e) Peaks are separated by 10 nm ( $\lambda$ =900 nm and 910 nm).

Using the optimized  $Si_3N_4$  passive components, on-chip SHFTS is designed and simulated by Lumerical Interconnect simulations. The FTS consists of an array of 24 MZIs with linearly increasing path length difference  $\Delta L_i$  (i=1,2...24) (Fig. 2. (a)) and the compact S-parameter models of designed passive components were used to build the FTS in Interconnect simulation (Fig. 2. (b)). Fig. 2. (c) shows the overall FTS operation process; for a given input source, the phase change is converted into an intensity change based on interferometric schemes. The input spectrum can be retrieved through the discrete Fourier cosine transform (Eq. (1)) [1].

$$p^{in}(\bar{\sigma}) = \frac{\Delta x}{N} P^{in} + 2 \frac{\Delta x}{N} \sum_{i=1}^{N} F(x_i) \cos 2\pi \bar{\sigma} x_i, \text{ where } F(x_i) = \frac{1}{B_s} (2P_i^{out} - A_s P^{in})$$
 (1)

Here,  $\sigma$  is the wavenumber, and  $\bar{\sigma} = \sigma - \sigma_{min}$  is the shifted wavenumber, where  $\sigma_{min}$  represents the minimum wavenumber. The spatial interferogram  $F(x_i)$  is discretized at N equally spaced delay values  $x_i (0 \le x_i \le \Delta x)$ corresponding to the outputs of each MZIs, which is defined as  $x_i = n_{eff} \Delta L_i$ , where  $n_{eff}$  is the effective index of the strip waveguide and  $\Delta x$  is the maximum delay. The input power  $P^{in}$  is constant for all the MZIs, and  $P_i^{out}$  represents the output power of the ith MZI with the coupling and loss coefficients of the MZI components  $A_s$  and  $B_s$ . The resolution of spectrometers, represented by the wavenumber resolution  $\delta\sigma$  or wavelength resolution  $\delta\lambda$  is determined by the maximum interferometric delay  $\Delta x$  as following [1]:  $\Delta L_{max} = \frac{1}{\delta \sigma \cdot n_{eff}} \cdots$  (2), where  $\delta \sigma \approx \frac{\delta \lambda}{\lambda_0^2}$ . The number of MZIs in the array (N) is determined from the Fourier sampling theorem as follows:  $N_{min} = 2\Delta x \Delta \sigma = 2\frac{\Delta \sigma}{s\sigma}$  $2\frac{\Delta\lambda}{\delta\lambda}$ ... (3), where  $\Delta\sigma$  and  $\Delta\lambda$  are the wavenumber and wavelength spectral range of the spectrometer. Based on Eq.(2) & (3), targeting SHFTS with  $\delta\lambda = 5$  nm,  $\Delta\lambda = 60$  nm at the center wavelength  $\lambda_0 = 900$  nm, we designed N=24 and  $\Delta L_{max} = 106 \,\mu m$  MZI array and simulated with various input spectrums to verify the device. MATLAB was used for data processing to retrieve the input spectrum based on Eq. (1). We put two lasers to generate input spectrums with two peaks separated by 5 nm and 10 nm to validate the resolution of the spectrometer. Fig. 2. (d) and (e) show the FTS results which show a good matching between input and retrieved spectrums. Because the FTS is designed to have a 5 nm resolution, two peaks were retrieved successfully, but there is a discrepancy of input and retrieved spectrum in between 900~905 nm in Fig. (2). (d). In summary, an on-chip SHFTS on Si<sub>3</sub>N<sub>4</sub>-on-SiO<sub>2</sub> is designed and demonstrated using an array of MZIs. The device fabrication and experimental study are in progress.

The research was supported by the Air Force Research Laboratory Contract # FA864920P0971.

#### References

- [1] M. Florjańczyk, et al., Opt. Express 15, 18176-18189 (2007)
- [2] E. Heidari, et al., Opt. Lett. 44, 2883-2886 (2019)
- [3] M. M.-Ballester, et al., Sci Rep 9, 14633 (2019)
- [4] S. K. V. Sekar, et al., PLoS ONE 11(12) (2016)
- [5] S. Liu, et al., Sensors 18, 3203 (2018)
- [6] P. Muñoz, et al., Sensors 17, 2088 (2017)



What Starts Here Changes the World

# On-Chip Si<sub>3</sub>N<sub>4</sub> Spatial Heterodyne Fourier Transform Spectrometer for the Optical Window in Biological Tissue

Kyoung Min Yoo<sup>1</sup> and Ray T. Chen<sup>1,2</sup>

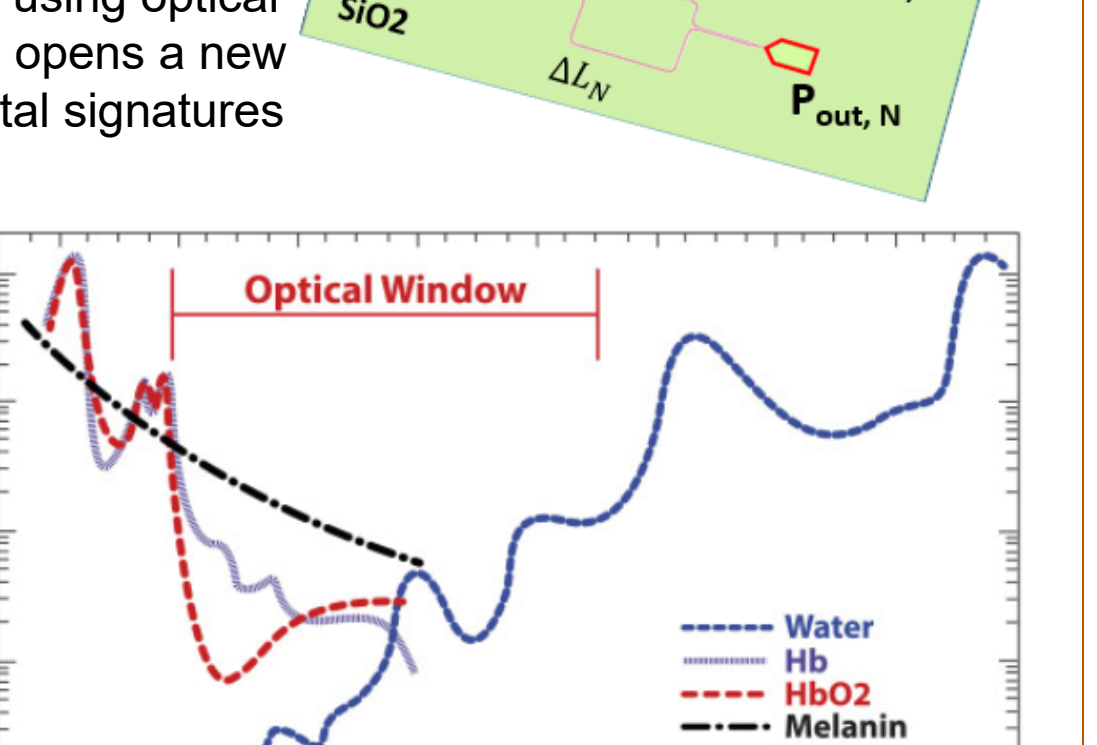
<sup>1</sup> Department of Electrical Engineering, University of Texas at Austin, 10100 Burnet Rd, Building 160, Austin, Texas 78758, U.S.A.





#### ntroduction

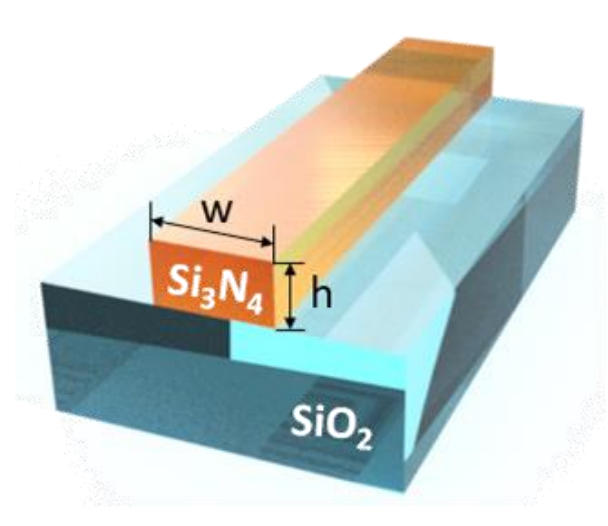
- Spatial Heterodyne Fourier Transform
  Spectrometer (SHFTS) consists of an array of
  Mach-Zehnder interferometer (MZI) with linearly
  increasing optical path delays implements onchip miniaturized spectrometer [1].
- A non-invasive in vivo diffuse optical characterization of human tissues using optical spectroscopy in  $\lambda$  =600~1200 nm opens a new possibility of monitoring various vital signatures of users [2].
- Silicon nitride (Si<sub>3</sub>N<sub>4</sub>)
   waveguide with silicon
   dioxide (SiO<sub>2</sub>) cladding has
   low material absorption
   losses across this
   wavelength range [3].

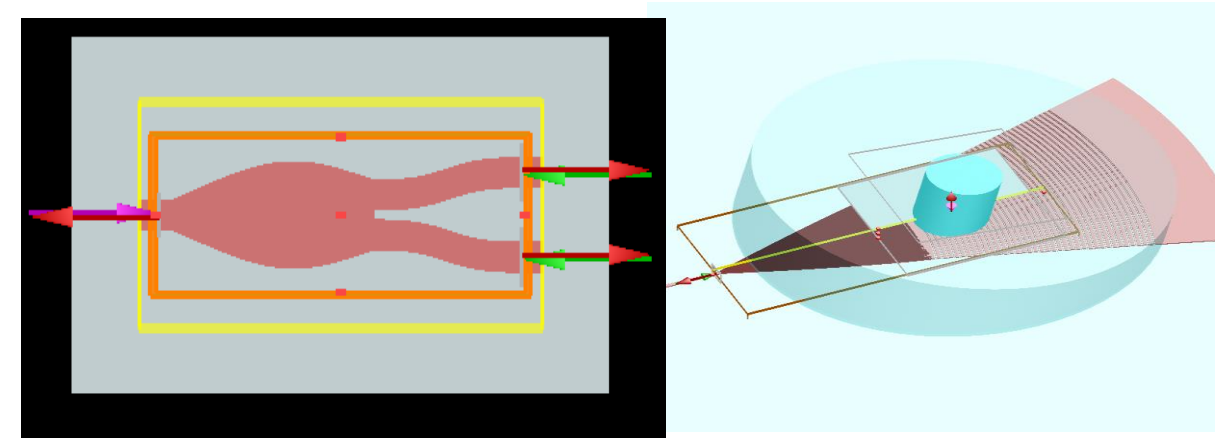


wavelength (nm)

#### Methods

The passive components including single mode  $Si_3N_4$  strip waveguide, Y-branch and sub-wavelength grating couplers are designed and optimized for the low-loss operation in the wavelength region of  $\lambda = 600 \sim 1000$  nm using Lumerical 3D mode and FDTD simulations.





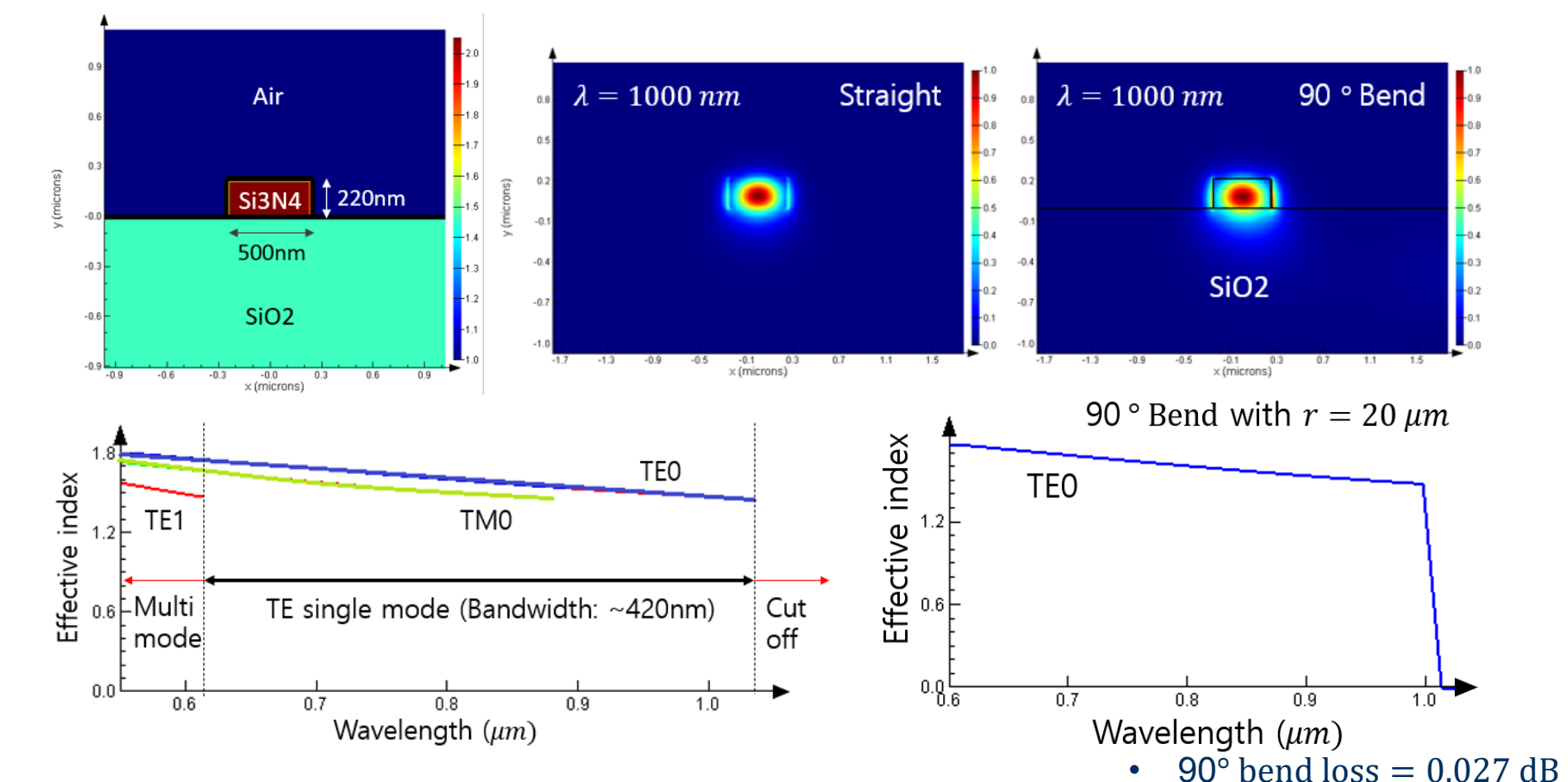
The input spectrum can be retrieved from the interference pattern at the MZI output powers through the discrete Fourier transform, and the resolution and bandwidth of spectrometer are determined by the maximum interferometric delay and the Fourier sampling theory [1].

$$p^{in}(\bar{\sigma}) = \frac{\Delta x}{N} P^{in} + 2 \frac{\Delta x}{N} \sum_{i=1}^{N} F(x_i) cos 2\pi \bar{\sigma} x_i$$
, where  $F(x_i) = \frac{1}{B_S} (2P_i^{out} - A_S P^{in}) \cdots$  [Eq. 1]  $\sigma = \frac{1}{A}$ : wavenumber;  $\bar{\sigma} = \sigma - \sigma_{min}$ : Shifted wavenumber;  $x_i = n_{eff} \Delta L_i$ : Modified delay

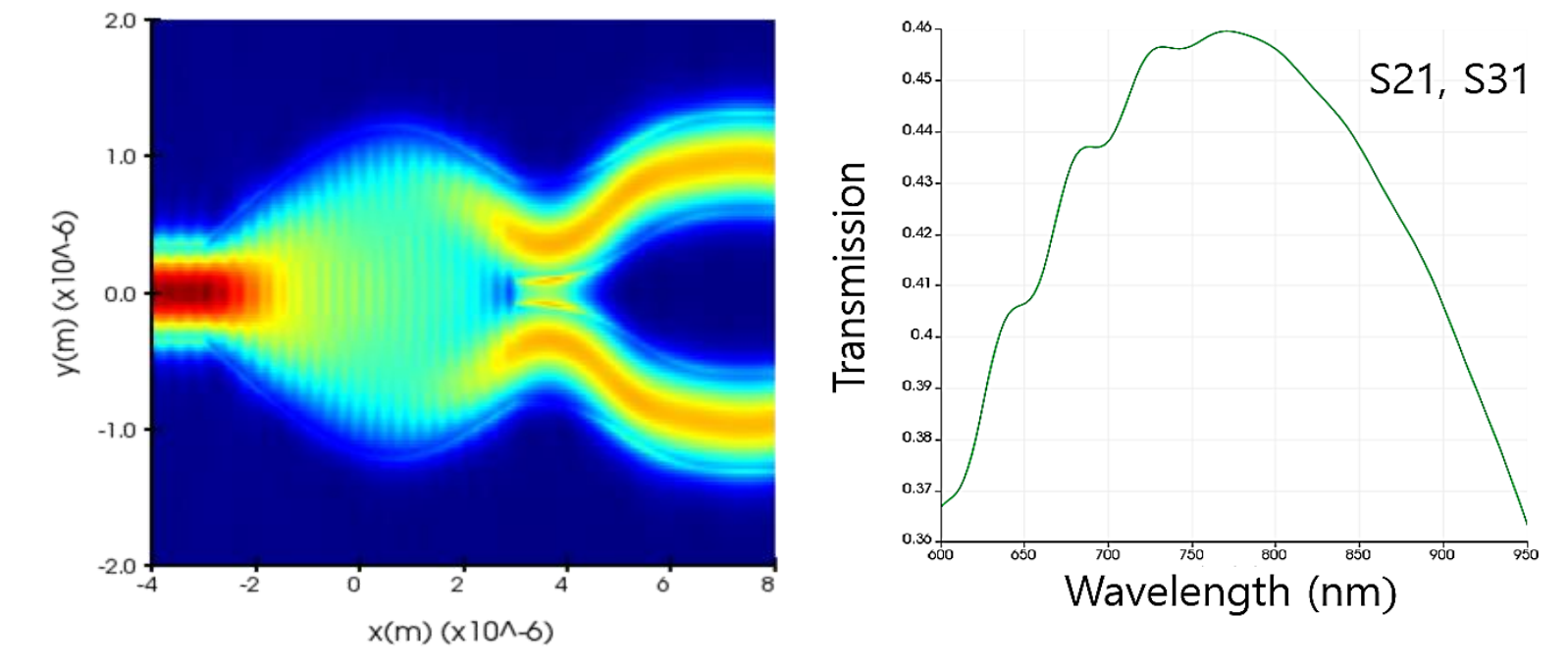
- Maximum interferometric delay:  $\Delta L_{max} = \frac{1}{\delta \sigma \cdot n_{eff}}$
- The minimum number of MZI:  $N_{min} = 2\Delta x \Delta \sigma = 2\frac{\Delta \sigma}{\delta \sigma} = 2\frac{\Delta \lambda}{\delta \lambda}$
- Using the optimized components, SHFTS parameters are designed based on the theoretical design principles and simulated by Lumerical Interconnect simulation to have the resolution of  $\delta\lambda \cong 5~nm$  and bandwidth of  $\Delta\lambda \cong 60~nm$ .

## Simulations and Designs

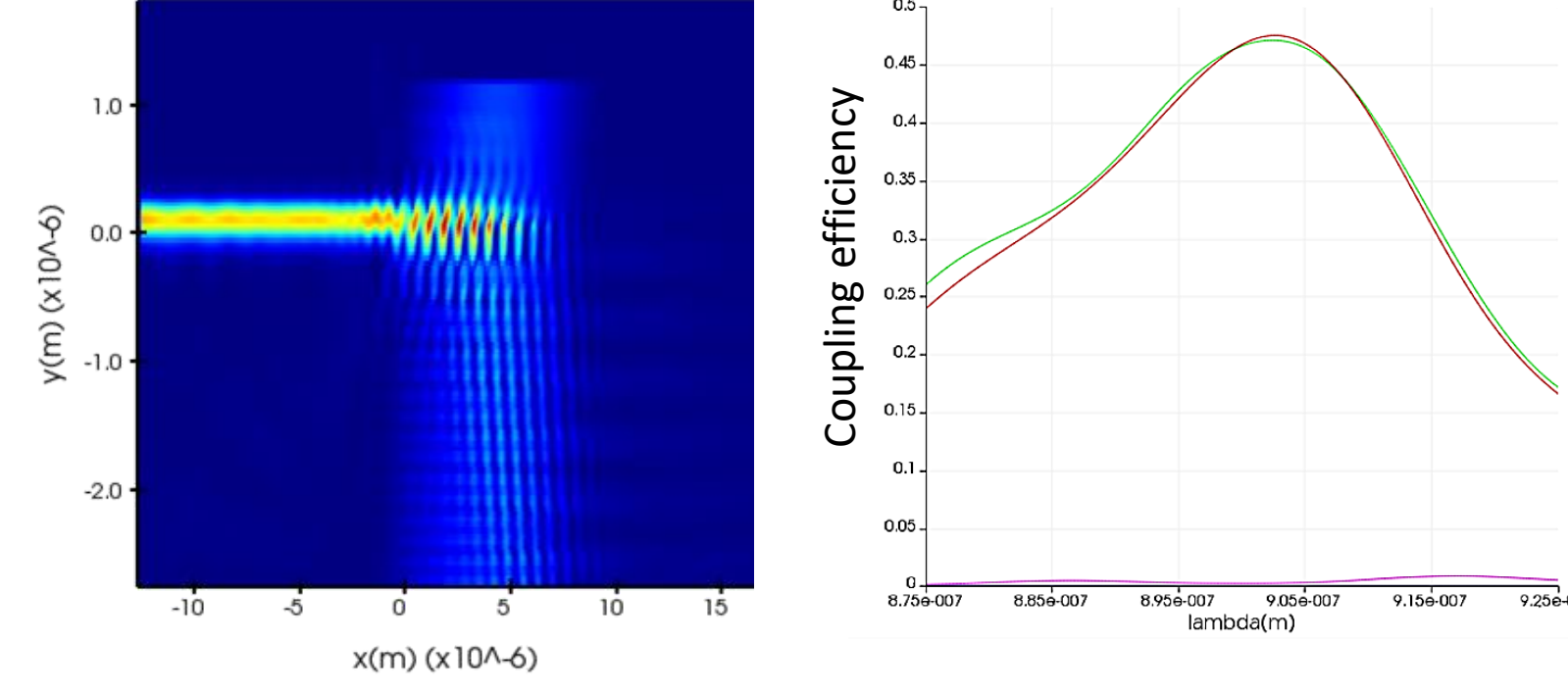
• The dimensions of the  $Si_3N_4$  strip waveguide and bend radius are optimized to allow low-loss single TE mode in the wavelength region of  $\lambda = 600 \sim 1000$  nm.



The low-loss Y-branch and grating coupler (GC) are designed and optimized to build the MZI array and effectively couple the light in and out from the waveguide. Sub-wavelength design is implemented to minimize the Fresnel back reflection and achieve fully-etching GC design.



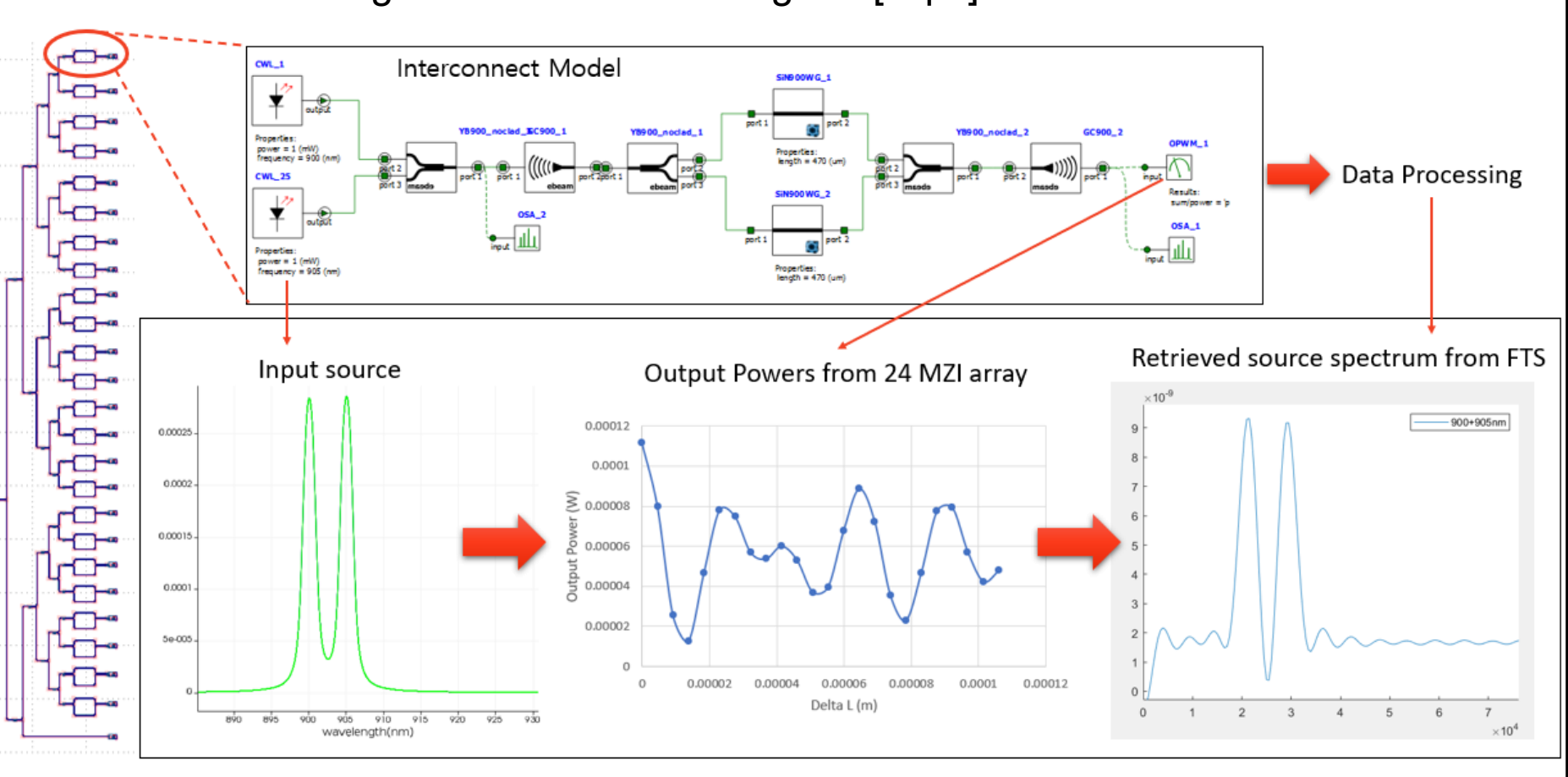
• Y-splitter loss: ~0.4 dB @  $\lambda$  =800nm; ~0.9 dB @  $\lambda$  = 900nm



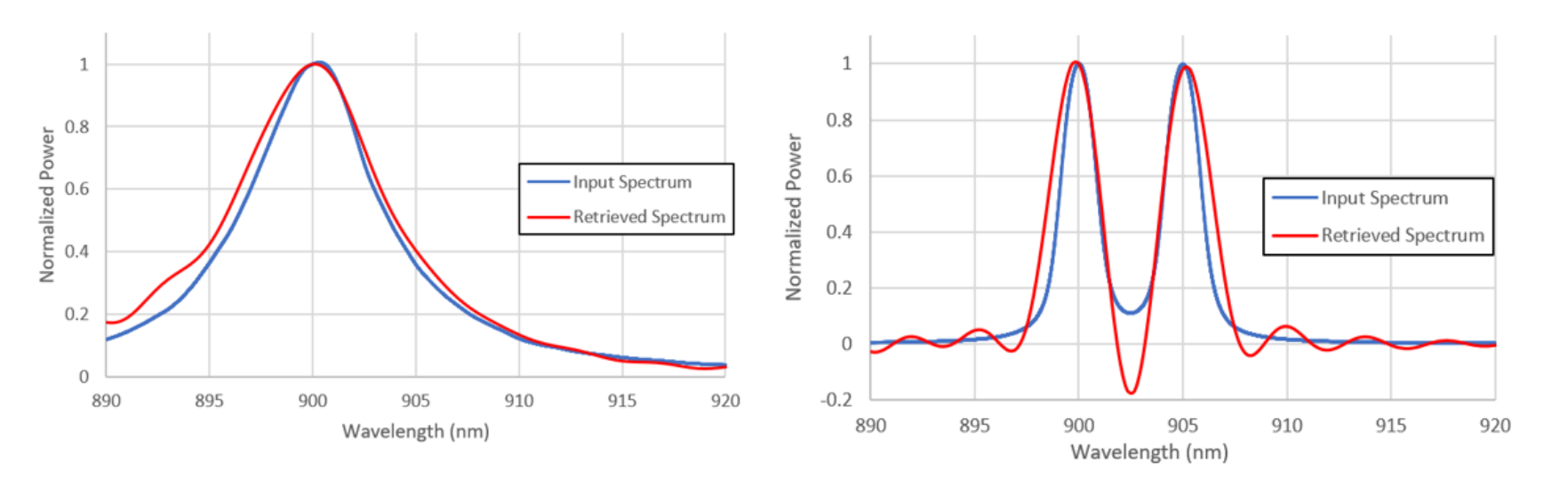
- TE mode Coupling loss: 3.3 dB @  $\lambda$  = 900 nm
- We designed SHFTS as N=24 and  $\Delta L_{max}$ =106 μm to achieve  $\delta \lambda \cong 5$  nm and  $\Delta \lambda \cong 60$  nm, and verified the performance using the optimized components' S-parameters in the interconnect simulation.

#### Results

 Overall interconnect simulation flow and results. The input spectrum was retrieved through MATLAB code using the [Eq.1]

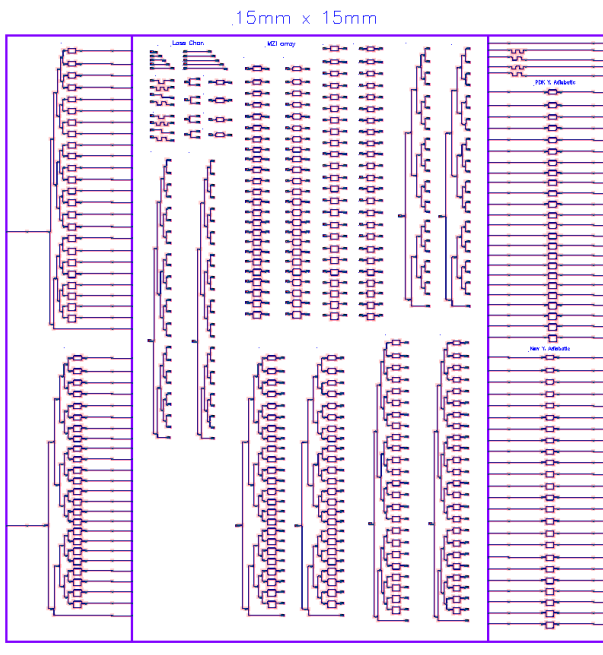


Successfully retrieved the input spectrum with the resolution of ~5nm.



#### **Conclusion and Future Work**

- o An on-chip SHFTS for  $\lambda$  =600~1000 nm is designed using Si<sub>3</sub>N<sub>4</sub>-on-SiO<sub>2</sub> platform. Low-loss passive components are designed and optimized to build MZI array, and the spectrometer performance with  $\delta\lambda \cong 5~nm$  and  $\Delta\lambda \cong 60~nm$  is demonstrated using the optimized passive components and interconnect simulations.
- The device fabrication and experimental study including broadband operation will be demonstrated in the next publications.



### Reference & Acknowledgements

- [1] M. Florjańczyk, et al., Opt. Express 15, 18176-18189 (2007)
- [2] S. K. V. Sekar, et al., PLoS ONE 11(12) (2016)
- [3] P. Muñoz, et al., Sensors 17, 2088 (2017)

The research was supported by the Air Force Research Laboratory Contract # FA864920P0971